Journal of Applied Polymer Science

Nanoindentation Measurements of Teflon-AF Nanosheets

Ina Rianasari,[1] James Weston,[2] Reza Rowshan,[2] Thomas Blanton,[3] Sachin Khapli,[1] Ramesh Jagannathan[1]

[1]Engineering Division, New York University, Abu Dhabi, UAE
[2]Core Equipment Facility, New York University, Abu Dhabi, UAE
[3]International Centre for Diffraction Data, 12 Campus Boulevard, Newtown Square, Pennsylvania 19073-3273
Correspondence to: R. Jagannathan (E-mail: rj31@nyu.edu)

ABSTRACT: We report the formation of cohesive, mechanically robust thin films of Teflon-AF formed via self-assembly of nanoparticles at both air/water and oil/water interfaces of micro-emulsion droplets. We also present results of morphological and mechanical investigations of thin films formed at these oil/water interfaces. Scanning electron microscope and low angle X-ray diffraction characterization of drop cast thin films from the micro-emulsions showed the presence of stacks of nanosheets with an average thickness of 6 nm. Atomic force microscopy (AFM) characterization put the thickness at a much lower value of around 2 nm implying that these sheets are comprised of molecular sheets of Teflon-AF. AFM characterization also indicated that these sheets are stretched molecular films comprising inter-diffused molecular chains, arranged in a regular fashion. Nanoindentation studies of these films unambiguously demonstrated the "tablet sliding" mechanism, similar to nacre, for dissipating applied stress. © 2014 Wiley Periodicals, Inc. J. Appl. Polym. Sci. **2015**, *132*, 41360.

KEYWORDS: amorphous; mechanical properties; properties and characterization

Received 31 May 2014; accepted 31 July 2014
DOI: 10.1002/app.41360

INTRODUCTION

Amorphous Teflon (Teflon-AF) is a class of fluoropolymers prepared by copolymerization of 4,5-difluoro-2,2-bis (trifluoromethyl)-1,3-dioxole (BDD) and tetrafluoroethylene (TFE) (Figure 1). Designed at the molecular level, these materials are well known for their outstanding optical, electrical, and mechanical properties combined with excellent chemical inertness and biocompatibility.[1,2] In these macromolecules, the introduction of bulky dioxole moieties to a PTFE backbone results in an amorphous structure with a large fractional free volume.[3] The high free volume combined with the amorphous structure imparts better mechanical and optical properties to the material[1,4] as compared to the microcrystalline Teflon polymer. Teflon-AF materials exhibit interesting mechanical properties such as high compressibility, high creep resistance to tensile and compressive loads, and low coefficient of friction. These properties combined with their excellent thermochemical resistance, low dielectric constant, and high gas permeability enable several applications of the material across the semiconductor,[5] optoelectronic,[6] and biomedical industries.[7] Nanoscale coatings of Teflon-AF are used in waveguides,[8] antireflective coatings,[9] low-k dielectric films in semiconductor devices,[10] and antifouling surfaces in microfluidic devices.[11] Knowledge of the mechanical properties of Teflon-AF films at nanoscale spatial resolution is therefore necessary for the design of such devices.

The technique of nanoindentation has been well developed over the past decade and applied to the mechanical characterization of thin films with thickness in the nanoscale regime.[12–16] In this method, an indenter is allowed to make contact with the surface of interest and pressure is gradually applied while monitoring the depth of penetration. From the load–displacement (P-δ) curves it is possible to determine several mechanical properties of interest such as the hardness, elastic modulus, yield stress, and viscoelastic properties for thin films immobilized on a rigid substrate. The method has been applied for measurement of thin-film properties of metallic, ceramic, semiconductor, and polymeric materials, with international standard procedures[17,18] being applied for the analysis. Nanoindentation measurements of ultrathin polymeric films are complicated by several factors such as the range of soft loads required, viscoelastic/plastic nature of the indentation response, anisotropic nature of the properties due to polymer microstructure and continue to be an active area of research.

Additional Supporting Information may be found in the online version of this article.

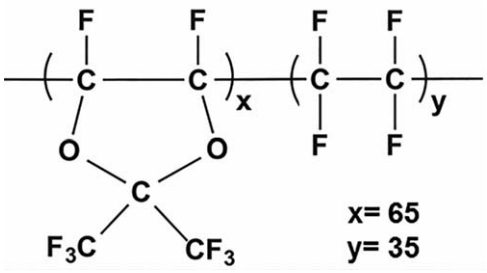

Figure 1. Molecular structure of Teflon-AF 1600 copolymers.

We have recently developed supercritical CO_2 based processing methods for creating nanoparticles and thin films of Teflon-AF using environment-friendly methods.[19] It has been demonstrated that nanoparticles (10–100 nm) can be collected in high yield and dispersed in either organic solvents (acetone, ethanol, and *n*-heptane) or at the air–water interface to create thin films. These films are found to be mechanically robust, stretchable, and superhydrophobic in nature. In this article, we report the results of nanoindentation studies of Teflon-AF films and compare the properties with corresponding films obtained by processing of Teflon-AF in a fluorinated solvent, Novec™ 7100 (i.e., methoxy-nonafluorobutane). Films obtained by the latter method are not superhydrophobic and lack the surface roughness and porous microstructure observed in the films prepared by supercritical fluids based processing of Teflon-AF.

EXPERIMENTAL

Materials

Teflon®-AF 1600 was procured from the DuPont™ Corporation (Wilmington, Delaware) in an amorphous resin form and used without further purification. Novec™ HFE 7100 (methoxy-nonafluorobutane) was obtained from 3M Specialty Materials, St. Paul, Minnesota. It consists of a mixture of isomers of methoxy-nonafluorobutane in unknown proportion. De-ionized water with an electrical resistance of 18.2 MΩ cm was used to prepare all aqueous solutions. Liquid carbon dioxide with purity of 99.9% was used to create the supercritical fluid medium for dissolution. Silicon wafers (100) orientation, polished, 380 μm (prime grade) were purchased from University Wafers Inc. (South Boston, USA) and cut into 1 cm × 1 cm pieces for sample preparation.

Rapid Expansion of Supercritical Solution Process

Formation of surfactant-free dispersions of Teflon-AF, formation of free-floating films on water, and solution processing of Teflon-AF in Novec™ HFE 7100 solvent have been previously reported.[19]

Emulsification and Film Formation

A free-floating Teflon-AF film formed on a water surface was sonicated after adding a cyclohexane layer on top (volume ratio of cyclohexane : water = 1 : 10). Sonication was performed using a Branson 250 Sonifier (tub sonicator) for 30 min at room temperature in a covered beaker. Films were formed on clean Si wafers by air-drying drop cast solutions of emulsion droplets at room temperature.

Optical Microscopy and Raman Imaging

Optical and Raman microscopy was performed on a WiTec alpha 300 confocal Raman microscope equipped with ×50 and ×100 objectives. The pinhole diameter of the confocal microscope was kept constant at 100 μm. Raman spectra were acquired using 488 nm laser for excitation (10 mW power) and recorded using a CCD camera maintained at -60°C. Integration time for acquisition of spectra was kept constant at 1 s. Each spectrum is an average of 10 consecutive scans. Teflon-AF films were rescanned after data acquisition to detect radiation-induced damage. No chemical change in the film composition was detected for an exposure time of 10 s at 10 mW power.

Scanning Electron Microscopy

Scanning electron microscopy (SEM) images of Teflon-AF polymeric films immobilized on solid substrates were obtained using a FEI Quanta FEG 450 electron microscope (acquired at 5–20 kV accelerating voltage and 10^{-3} to 10^{-4} Pa pressure).

Nanoindentation Experiments

The nanoindentation experiments were performed using an Agilent G200 Instrumented Indentation Testing (IIT) nanoindenter, equipped with a diamond Berkovich indenter with a radius less than 20 nm. The system is in compliance with ISO 14577. Traditional hardness testing yields only one measure of deformation at one applied force, whereas during an IIT test, force and penetration are measured for the entire time that the indenter is in contact with the material. Instrumented indentation testing is particularly well suited for measuring Young's modulus (E) and hardness (H) of material such as thin films, particles, or other small features.

In the current study, we used two methods to conduct nanoindentation, namely, basic hardness testing with continuous load–displacement data and Continuous Stiffness Measurement (CSM). For the basic hardness, the indenter was loaded at a constant rate until reaching the specified peak load, hold for specific time, and then unloaded at the same rate. The steps for reaching the maximum load can also be specified during the tests. The CSM option allows the continuous measurement of the contact stiffness during loading and is not just at the point of initial unload. This was accomplished by superimposing a small oscillation on the primary loading signal and analyzing the resulting response of the system by means of a frequency-specific amplifier. With the continuous measure of contact stiffness, one obtains the hardness and elastic modulus as a continuous function of depth from a single indentation experiment.

The samples for both methods were mounted on aluminum disks using Crystalbond™, a thermoplastic polymer, and loaded to the sample tray capable of holding up to four samples at the same time. The nanoindentation system was placed on a vibration isolation table and it is equipped with a ×10 and ×40 objectives making it possible to adjust the height of the samples using the reference sample, Corning 7980 (fused silica), located at the center of the sample tray. During each experimental batch, we also ran control experiments with a fused silica sample to ensure quality control, keep track of the performance of the instrument, and indirectly verify proper operation according to ISO-14577. All experiments were conducted at room temperature.

The system specifications for the nanoindenter are as follows: displacement resolution: < 0.01 nm, total indenter travel:

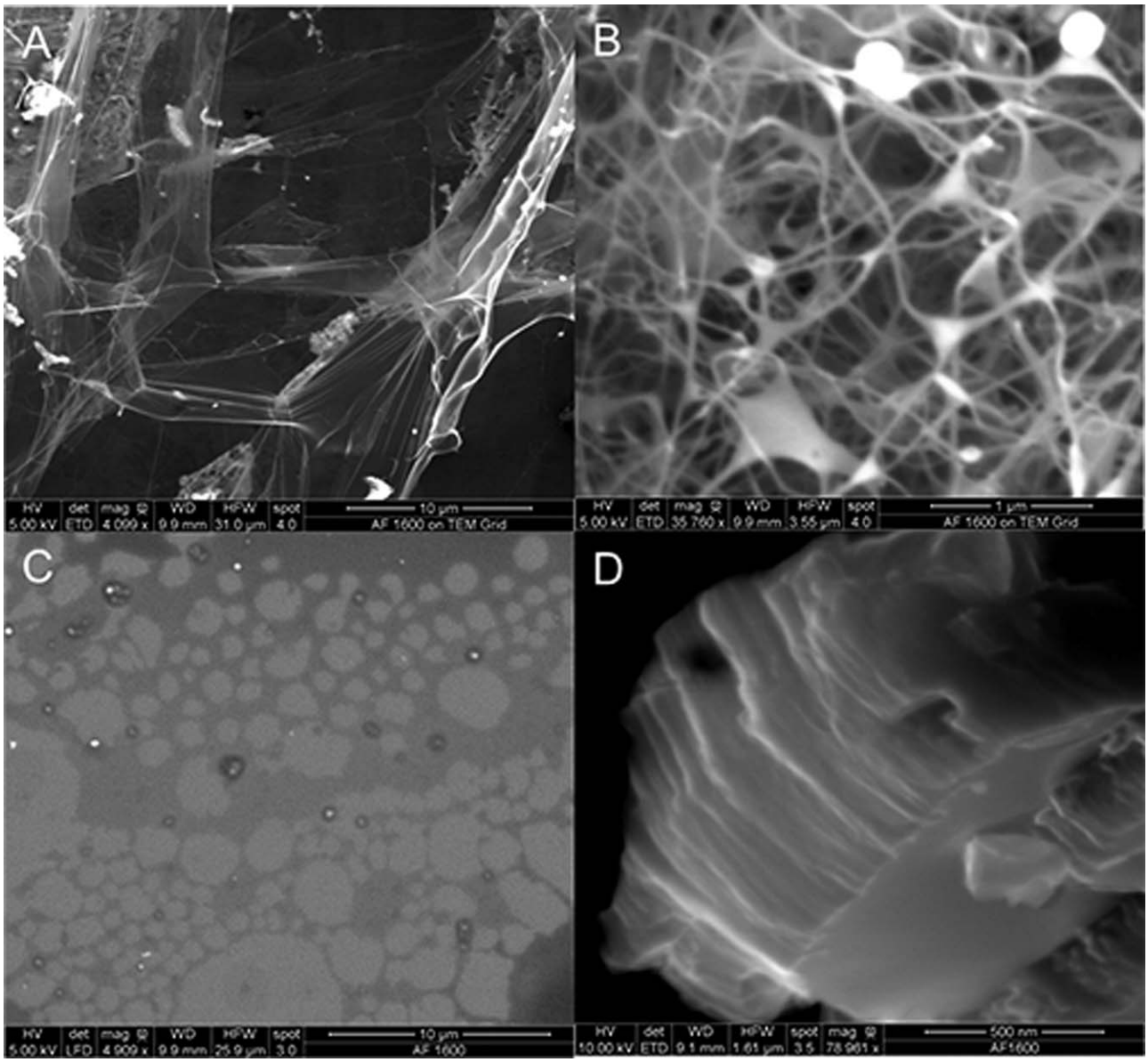

Figure 2. SEM micrographs of free nanosheets of Teflon-AF on copper grid (A, B) and drop-casted film from emulsion on silicon substrate (C). Molecular stacks of drop-casted emulsion film (D).

1.5 mm, maximum indentation depth: >500 μm, load application: coil/magnet assembly, displacement measurement: capacitance gauge, maximum load (standard): 500 mN, load resolution: (XP) 50 nN, contact force: <1.0 μN, load frame stiffness: $\sim 5 \times 10^6$ N m^{-1}, and software: NanoSuite.

X-ray Diffraction Experiments

Samples were measured using a Panalytical Empyrean diffraction system using Cu Kα radiation (1.5418 Å). The samples were irradiated using a parallel beam focusing mirror, 0.04 radian Soller slits, and a 0.27° parallel slit collimator placed before the scintillation detector. The samples were aligned for X-ray reflectivity, with the sample blocking half the incident intensity and symmetric reflection geometry ($\omega = \theta$). Step scan measurements were made with a step size of 0.01° 2θ and a count time of 16 s step^{-1}.

Atomic Force Microscopy Experiments

Atomic force microscopy (AFM) measurements were carried out in intermittent mode in air using Agilent MAC Mode III module. We used silicon Point Probe Plus cantilevers (Nanosensors, Switzerland) with a resonant frequency of 330 kHz and spring constant of 42 N m^{-1}. Height, phase, and amplitude images were acquired simultaneously. The images were further analyzed by using Gwyddion free software.

RESULTS AND DISCUSSIONS

Free-standing films of Teflon-AF were created by the rapid expansion of supercritical solution process at the air–water interface. Electron micrographs [Figure 2(A,B)] of samples of this film drop cast on a copper grid and dried at room temperature show evidence of mechanically robust, extremely thin sheets of Teflon-AF.

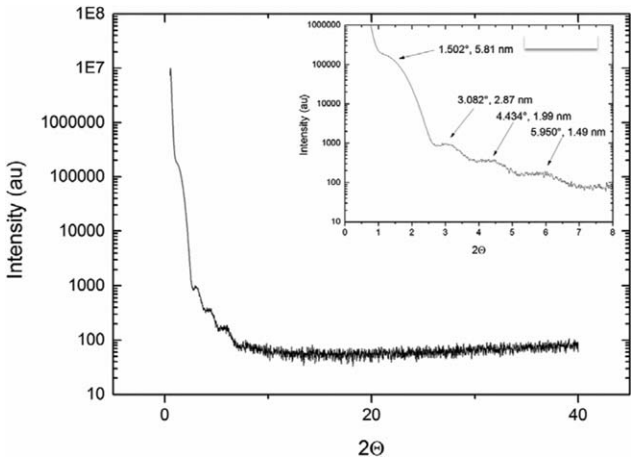

Figure 3. XRD diffraction pattern of drop casted emulsion Teflon-AF thin film.

We used the emulsification process to further increase the specific surface area of these films and the oleophilic nature of these films was expected to drive their spontaneous self-assembly at the oil–water interface. The electron micrographs of this film, drop-cast on a silicon substrate and dried at room temperature, are shown in Figure 2(C) and appear to support the notion of film formation by the drying of coalesced emulsion droplets. At the oil–water interface, the surface tension forces are expected to further stretch the films resulting in the formation of stacked layers of nanosheets which are clearly evident in the electron micrograph shown in Figure 2(D). The image shown in Figure 2(D) is from the same film sample shown in Figure 2(C) but from an area where two pieces have broken off from the main film thereby exposing the sliced inner surface. Results from low angle X-ray diffraction (XRD) characterization of the same film sample are presented in Figure 3. Low angle peaks at near equiangular $\Delta 2\theta$ are consistent with multiple order diffraction peaks (1st, 2nd, 3rd, 4th order), and combined with the SEM data in Figure 2(D), indicate the presence of a uniform thickness layered component. The absence of diffraction peaks at higher 2θ angles confirms the amorphous nature of the Teflon-AF thin film. Calculation of the interplanar *d*-spacings for the low angle diffraction peaks multiplied by the order of the corresponding diffraction peak gives an average nanosheet layer thickness of 5.9 ± 0.1 nm.

AFM examination of this film further validated the electron micrograph observations and the low angle XRD data. The

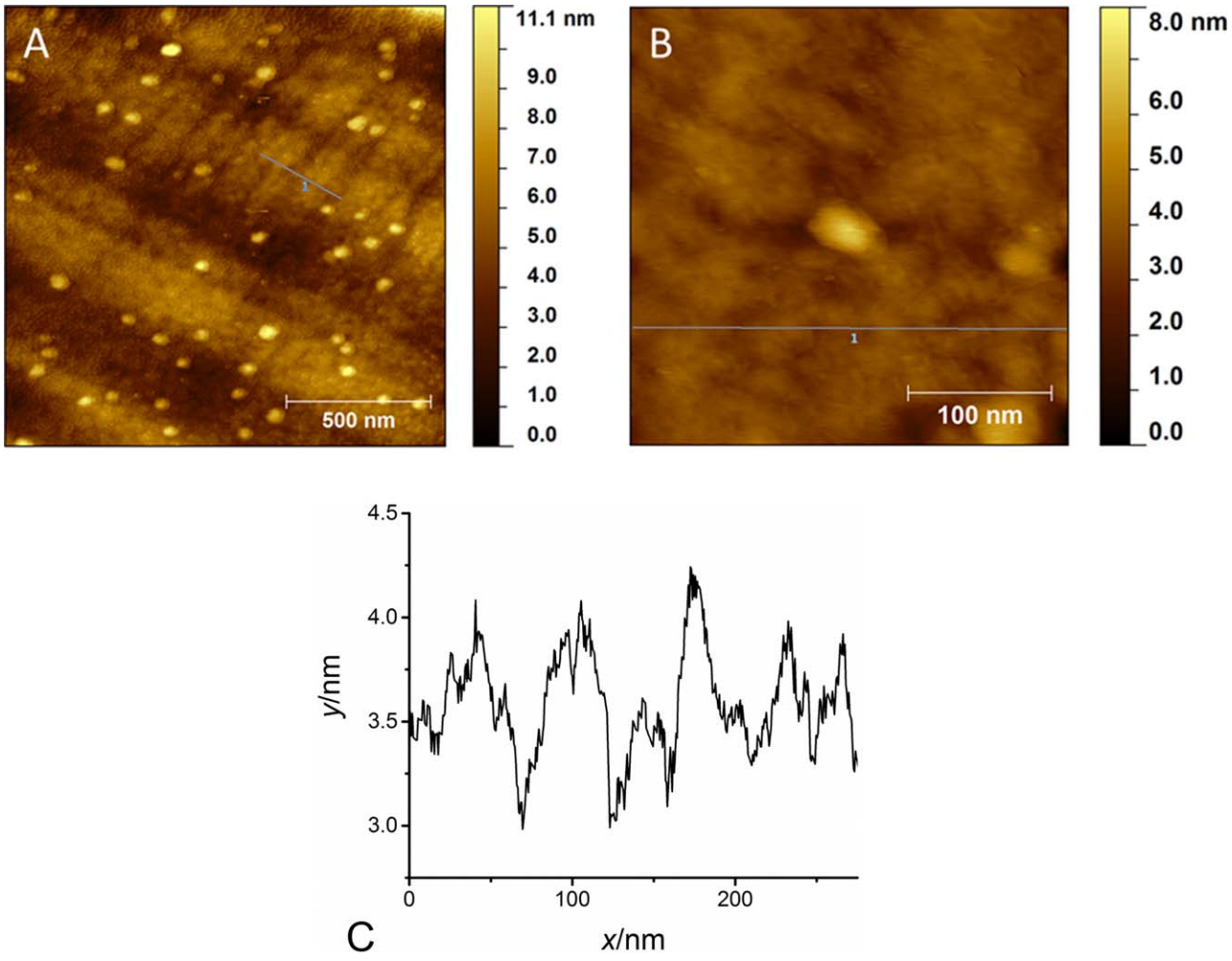

Figure 4. AFM images of emulsified Teflon-AF drop casted on silicon substrate. Topography of tapping mode AFM (A,B) and height profile of molecular chain shown in B (C). [Color figure can be viewed in the online issue, which is available at wileyonlinelibrary.com.]

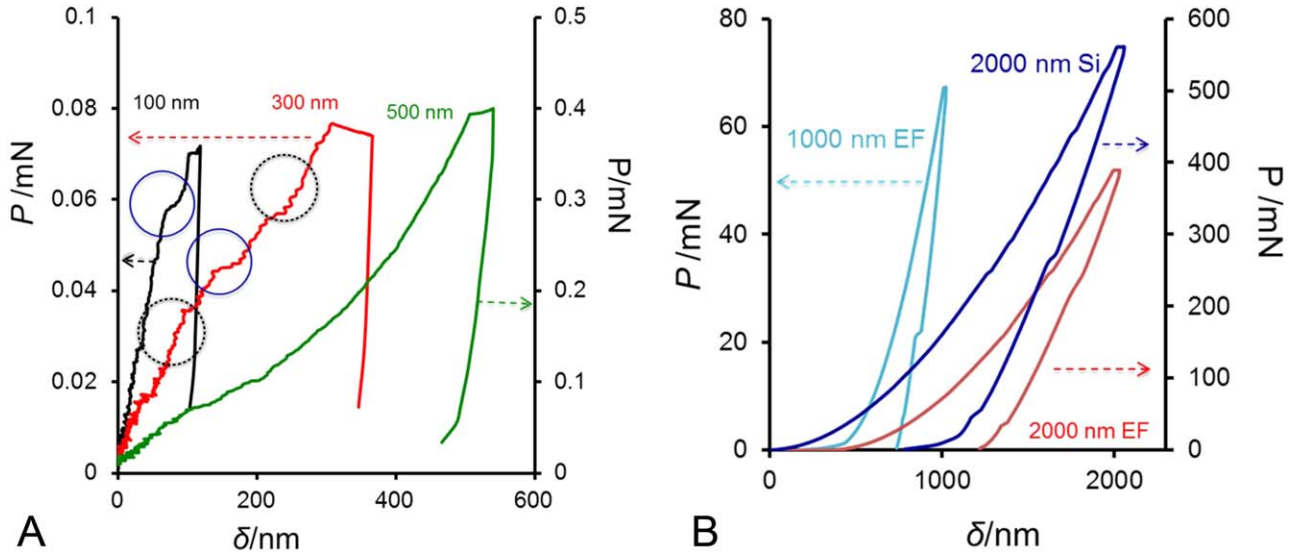

Figure 5. Load–displacement curves of different penetration depths. Low depth indentation of emulsion Teflon-AF thin film (A). High depth indentation of emuslion Teflon-AF thin film and uncoated silicon substrates (B). [Color figure can be viewed in the online issue, which is available at wileyonlinelibrary.com.]

results shown in Figure 4(A,B) indicate the presence of self-assembled, ordered arrays of Teflon-AF nanostructures. A higher magnification scan of the film revealed ordered arrays of molecular coils of Teflon-AF nanostructures implying nucleation of entangled molecular structures at the oil/water interface during the self-assembly process. This structure was not observed for (drop-cast) Teflon-AF from its solution in the solvent Novec^{TM} (see Supporting Information Figure S2) which is consistent with other published literature.[20] The height of these structures is approximately 1.0 nm indicating a sheet width of 2 nm, implying the presence of molecular sheets of Teflon-AF [Figure 4(C)].[20,21]

Mechanical characteristics of the Teflon-AF thin films created by our emulsion process, hereafter referred to as the Teflon-AF nanosheets, were studied by using the nanoindentation method. All the measurements were made on films, which were solution cast on a silicon substrate. Micro-Raman analysis was used for characterization of the solution cast films and the film composition was found to be uniform throughout the coated areas (Supporting Information Figure S1). To ensure intrinsic reliability, the measurements were primarily carried out on carefully selected film areas, apparently of high quality (see Supporting Information Figure S3).

In thin film nanoindentation studies, it is generally accepted that the depth of penetration should not exceed 30% of the film thickness in order to avoid any substrate influence.[12] We avoided the substrate effect problem by first carrying out CSM studies on the Teflon-AF nanosheets with increasing, final depth of penetration and examining the *P-δ* curves for any signs of substrate effect.[12,22] The data were also compared with corresponding CSM data for bare silicon substrates. We then chose the film thickness region that is free of any substrate effect for our studies.

The results of our CSM studies are shown in Figure 5. In Figure 5(A), *P-δ* data for indention depths of 100 nm, 300 nm, and 500 nm for Teflon-AF nanosheet thin films are shown. In Figure 5(B), the *P-δ* data for indentation depths of 1000 nm and 2000 nm for Teflon-AF nanosheet films and 2000 nm Si are reported. Unlike 100 nm and 300 nm, a characteristically typical, *P-δ* curve is observed for 500 nm, 1000 nm, and 2000 nm Teflon-AF nanosheets films. The *P-δ* profile for these films appears to be qualitatively similar to that for Si and the peak load for the 2000 nm film is actually close to that for Si. It is clear that substrate effects begin to emerge above 500 nm (for an apparent film thickness of 2000 nm). We also carried out a similar set of experiments for the film formed from a 0.1 wt % solution of Teflon-AF dissolved in the Novec^{TM} solvent (see Supporting Information Figure S4). Unlike the Teflon-AF nanosheets, the *P-δ* profiles from CSM experiments for 50 nm, 100 nm, 200 nm, 300 nm, and 500 nm indentation depths for the Novec^{TM} film were qualitatively similar to each other and to Si, indicating a significant substrate effect even at 50 nm indentations.

Interestingly, the unloading profiles for 100 nm and 300 nm indentation depths [Figure 5(A)] also showed no elastic recovery, strongly implying that the Teflon-AF nanosheets film primarily undergoes plastic deformation. We further investigated this phenomenon in a series of constant load/unload experiments where a peak load of 1 mN was reached in 1, 2, 4, and 6 steps (Supporting Information: Figure S5). For comparison purposes, similar experiments were carried out for the film cast from the Novec^{TM} solution. The Teflon-AF nanosheets results shown in Figure 6(A) confirmed no elastic recovery during unloading in any of these experiments. In contrast, the films cast from the Novec^{TM} solution showed a typical unloading profile, with significant elastic recovery [Figure 6(B)]. This result leads us to the interesting conclusion that while Teflon-AF as a material could undergo elastic deformation, it does not, when structured as stacks of nanosheets by our emulsion process.

For the Teflon-AF nanosheets film, the *P-δ* profiles for the 100 nm and 300 nm indentations are not only qualitatively very

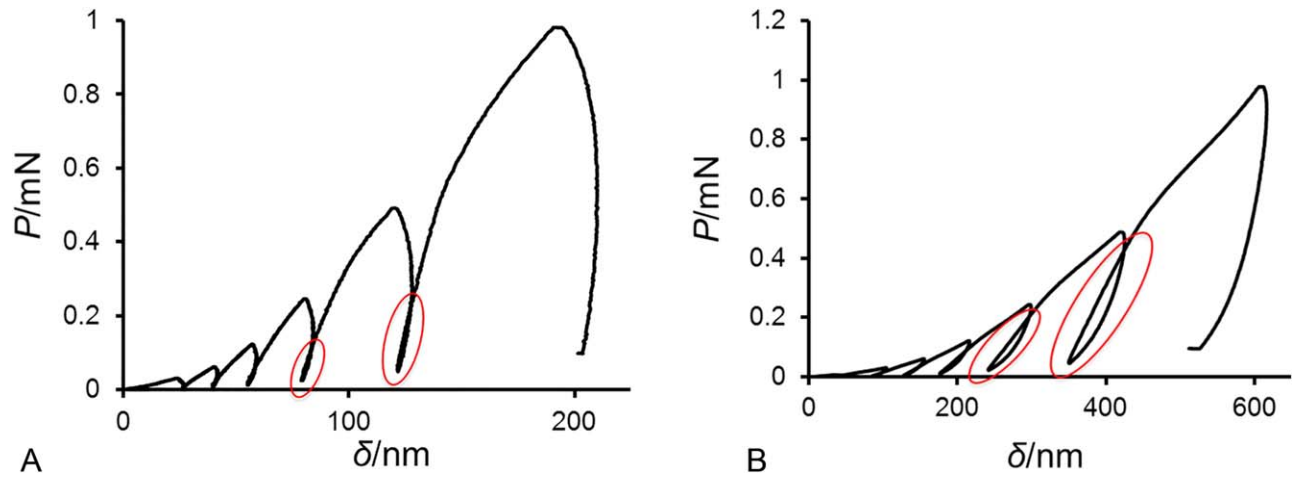

Figure 6. Non-elastic behavior of Teflon-AF drop casted from emulsion (A). Elastic behavior of dropcasted Teflon-AF drop casted from Novec™ solution (B). [Color figure can be viewed in the online issue, which is available at wileyonlinelibrary.com.]

different from that observed for 500 nm but the peak load for the 100 nm (70 mN) and 300 nm (74 mN) indentations are significantly lower than that for 500 nm (400 mN). More importantly, the 100 nm and 300 nm indentation *P-δ* curves also show significant "high" frequency perturbations (Figure 5, highlighted by dashed circles) in the loading profile, which are usually associated with dislocation activity in crystals due to plastic deformations.[23] Amorphous materials, such as this polymer film, by definition, do not have dislocations. We suspect that these high frequency perturbations are the response from the low-friction, nanosheets sliding against each other, like in a deck of cards, to dissipate the load applied to them. Since the rate of increase of applied load and the rate of dissipation by the sliding sheets are unbalanced, the tendency would be for the sheets to overreact to the applied load and then wait. This process would repeat itself in a cyclical fashion, which is what we observed.

It is also very likely that for any given loading rate profile, over a period of time, the sliding sheets are unable to effectively dissipate the load, leading to an accumulation of energy in the film and creation of "shear banding" (pop-in) events such as that observed in the *P-δ* profiles for 100 nm and 300 nm indentations [highlighted by the non-dashed circles in Figure 5(A)]. These are low frequency events. The high frequency perturbations continue to occur during these bigger "pop-in" events, as observed in the 300 nm profile. We observed these "pop-in" events in our constant load rate experiments as well, both during loading [Figure 7(A)] and during unloading [Figure 7(B)]. Similar "pop-in" events were observed in the nanoindentation studies on nacre and were referred to as "displacement jumps."[24] The mechanism for load dissipation via "tablet sliding" is well established in nacre and other biological specimens. The authors of this study attributed the "displacement jumps" to the collapse and densification of the tablet interfaces in nacre, during the tablet sliding process.[24] They also noted that they have to use high data acquisition rates to be able to see these "pop-ins."

We further investigated our hypothesis that Teflon-AF nanosheets film dissipates an applied load in a manner similar to the "tablets sliding" mechanism of nacre. As suggested earlier, if the high and low frequency oscillations of the *P-δ* profile are due to the imbalance between the applied loading rates and the sliding rates then we could test the validity of our hypothesis, if we are able to modulate this phenomenon of oscillations as a function

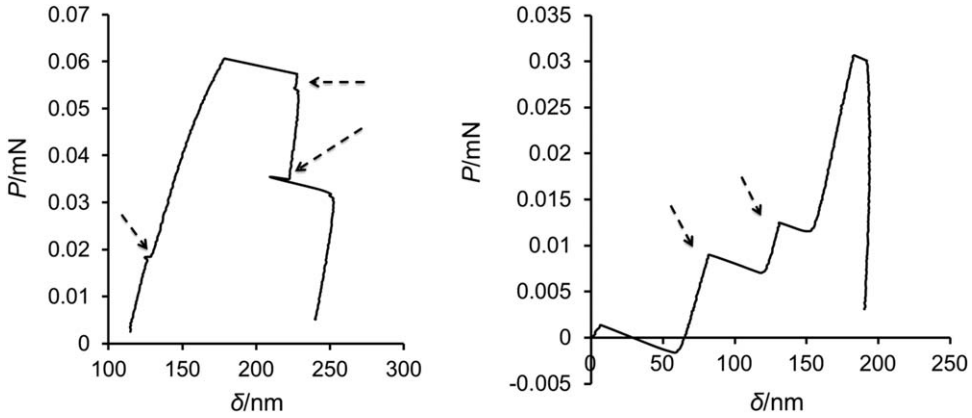

Figure 7. Low depth indentation of loading (A) and unloading (B).

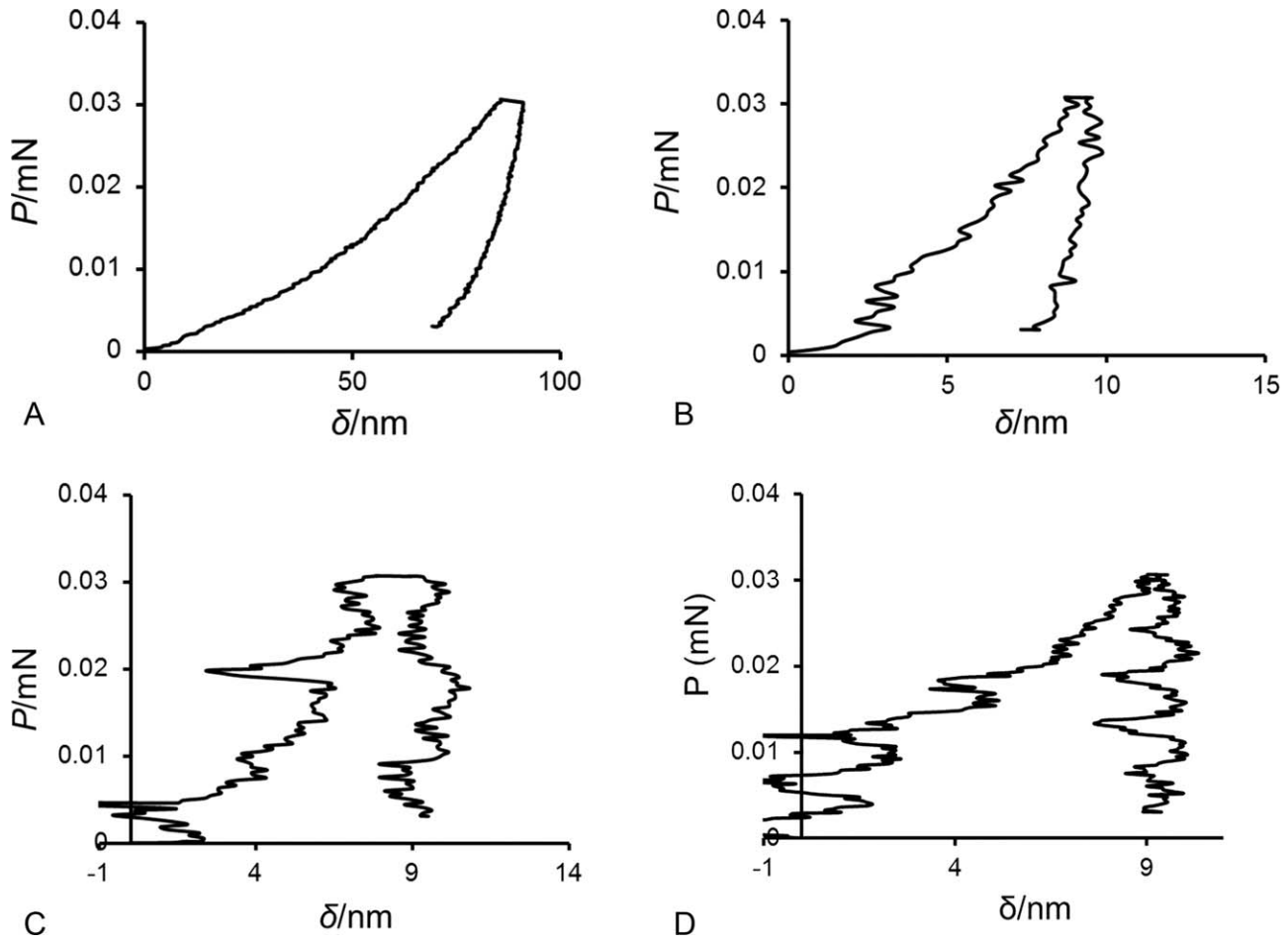

Figure 8. Penetration depth of solution cast Teflon-AF thin film (A). Different sliding behavior of emulsion Teflon-AF thin film depending on loading time: 10 s (B), 20 s (C), and 30 s (D).

of loading rates. In Figure 8, we show the results of the effect of loading rates on the *P-δ* profile, for a peak load of 30 μN. The results for Novec^{TM} film are shown in Figure 8(A) and interestingly, we do not see any low or high frequency oscillations for a loading rate of 1 μN s^{-1}. The signal to noise for the *P-δ* profile is excellent and proves that the instrument is capable of measuring the load and displacement values very precisely, in this range. The Teflon-AF nanosheets film data are shown in Figure 8(B–D). The data in Figure 8(B), for a loading rate of 3 μN s^{-1}, clearly shows the presence of the high frequency oscillations. We also note that significant sections of the *P-δ* profile did not show any high frequency oscillations. In Figure 8(C), for a slower loading rate of 1.5 μN s^{-1}, the entire *P-δ* profile is populated with high frequency oscillations. Moreover, we begin to see the emergence of the low frequency, "pop-in" features, both in the loading and unloading profiles. As we further decreased the loading rate to 1 μN s^{-1}, we were able to detect the high and low frequency oscillations throughout the entire *P-δ* profile. It is interesting to note that we are able to more clearly detect and record the oscillations as we decreased the loading rate from 3 μN s^{-1} to 1 μN s^{-1}. This result would suggest that, in the 1 μN s^{-1} to 3 μN s^{-1} range, nanosheets are apparently able to slide at rates that are needed to effectively dissipate the applied load. Apparently, at 3 μN s^{-1}, a majority of the high frequency sliding was outside the range of detectability of our instrument and hence not recorded. As we decreased the loading rate to 1.5 μN s^{-1} and 1 μN s^{-1}, the frequency range of "nanosheets sliding" decreased sufficiently to be within the detectability range of our instrument. This result would be consistent with the observations made by Barthelat et al who claimed that they had to use a high data acquisition rate to observe the so-called "displacement jumps" in their nacre specimens.[24] These results, therefore, unequivocally confirm our suggested mechanism of "sliding nanosheets" dissipating the applied load in our nanoindentation experiments. Our results thus prove that we are able to successfully create a physical system that mimics the "tablet sliding" nacre process.

CONCLUSIONS

Self-assembly of Teflon-AF nanoparticles on the cyclohexane/water interface resulted in the formation of stacks of mechanically robust, cohesive nanosheets at room temperature. SEM and low angle XRD results confirm the presence of a stacked sheets structure. While XRD results suggest an approximate film thickness of 5–6 nm, AFM results strongly suggest that these

nanosheets are molecular sheets of Teflon-AF. Nanoindentation studies on these nanosheets clearly demonstrated the phenomenon of "tablet sliding" that is usually associated with natural materials such as nacre. It is interesting to note the strong dependence of the sliding rate on the applied loading rate.

ACKNOWLEDGMENTS

This research is funded by New York University Abu Dhabi (nyuad.nyu.edu).

AUTHOR CONTRIBUTIONS

I.R. prepared samples and performed AFM analysis; J.W., R.R., and R.J. performed mechanical characterization using nanoindentation; J.W. acquired XRD data and T.B. helped interpret the data. S.K. performed Raman microscopy and optical imaging of the films. All authors discussed and contributed to the manuscript. The authors declare no competing financial interest.

REFERENCES

1. Zhang, H.; Weber, S. G. *Top Curr. Chem.* **2012**, *308*, 307.
2. Resnick, P. R.; Buck, W. H. In Fluoropolymers 2: Properties. Hougham, G. G.; Cassidy, P. E.; Johns, K.; Davidson, T., Eds.; Springer: New York, **1999**; Chapter *2*, p 25.
3. Hofmann, D.; Entrialgo-castano, M.; Lerbret, A.; Heuchel, M.; Yampolskii, Y. *Macromolecules* **2003**, *36*, 8528.
4. Yang, M. K.; French, R. H.; Tokarsky, E. W. *J. Micro/Nanolith. MEMS MOEMS*, **2008**, 7, *033010*(1).
5. Flückiger, R.; Lövblom,R.; Ostinelli, O.; Benedickter, H.; Bolognesi, C. R. *IEEE Electron Device Lett.* **2012**, *33*, 1135.
6. Mihailov, S.; Lazare, S. *Appl. Opt.* **1993**, *32*, 6211.
7. Bauer, S.; Schmuki, P.; von der Mark, K.; Park, J. *Prog. Mater. Sci.* **2013**, *58*, 261.
8. Cho, S. H.; Godin, J.; Lo, Y.-H. *IEEE Photon. Technol. Lett.* **2009**, *21*, 1057.
9. Bazin, N. J.; Andrew, J. E.; McInnes, H. A. In Proceedings of SPIE, Third International Conference on Solid State Lasers for Application to Inertial Confinement Fusion; Lowdermilk, W. H., Eds.; SPIE, Monterey, CA. **1999**; Vol. 3492, p 964.
10. Sharangpani, R.; Singh, R.; Drews, M.; Ivey, K. *J. Electron. Mater.* **1997**, *26*, 402.
11. Czolkos, I.; Hakonen, B.; Orwar, O.; Jesorka, A. *Langmuir* **2012**, *28*, 3200.
12. Bhushan, B.; Li, X. *Int. Mater. Rev.* **2003**, *48*, 125.
13. Van Landingham, M. R.; Villarrubia, J. S.; Guthrie, W. F.; Meyers, G. F. *Macromol. Symp.* **2001**, *167*, 15.
14. Zhang, C. Y.; Zhang, Y. W.; Zeng, K. Y.; Shen, L. *J. Mater. Res.* **2011**, *20*, 1597.
15. Strojny, A.; Xia, X.; Tsou, A.; William, W. *J. Adhes. Sci. Technol.* **2012**, *12*, 1299.
16. Ramamurty, U.; Jang, J. *Cryst. Eng. Comm.* **2014**, *16*, 12.
17. ASTM E2546-2007. Standard Practice for Instrumented Indentation Testing; ASTM International: West Conshohocken, PA.
18. ISO14577:2012. Metallic Materials-instrumented Indentation Test for Hardness and Materials Parameters; ISO Central Secretariat, 1 rue de Varembé, 1211: Geneva 20, Switzerland.
19. Khapli, S.; Jagannathan, R. *J. Supercrit. Fluids* **2014**, *85*, 49.
20. Tavana, H.; Jehnichen, D.; Grundke, K.; Hair, M. L.; Neumann, A.W. *Adv. Colloid Interface Sci.* **2007**, *134–135*, 236.
21. Gallyamov, M. O.; Vinokur, R. A.; Nikitin, L. N.; Said-Galiyev, E. E.; Khokhlov, A. R.; Yaminsky, I. V.; Schaumburg, K. *Langmuir* **2002**, *18*, 6928.
22. Pethica, J. B.; Oliver, W. C. *Mater. Res. Soc. Symp. Proc.* **1989**, *130*, 13.
23. Lund, A. C.; Hodge, A. M.; Schuh, C. A. *Appl. Phys. Lett.* **2004**, *85*, 1362.
24. Barthelat, F.; Li, C.-M.; Comi, C.; Espinosa, H. D. *J. Mater. Res.* **2011**, *21*, 1977.